Societal shifts due to COVID-19 reveal large-scale complexities and feedbacks between atmospheric chemistry and climate change

Joshua L. Laughner[a,1], Jessica L. Neu[b,1], David Schimel[b,1], Paul O. Wennberg[a,c,1], Kelley Barsanti[d], Kevin Bowman[b], Abhishek Chatterjee[e,f], Bart Croes[g,cc], Helen Fitzmaurice[h], Daven Henze[i], Jinsol Kim[h], Eric A. Kort[j], Zhu Liu[k], Kazuyuki Miyazaki[b], Alexander J. Turner[l,h,b], Susan Anenberg[m], Jeremy Avise[n], Hansen Cao[i], David Crisp[b], Joost de Gouw[o,cc], Annmarie Eldering[b], John C. Fyfe[p], Daniel L. Goldberg[m], Kevin R. Gurney[q], Sina Hasheminassab[r], Francesca Hopkins[s], Cesunica E. Ivey[d,t], Dylan B.A. Jones[u], Junjie Liu[b], Nicole S. Lovenduski[v], Randall V. Martin[w], Galen A. McKinley[x], Lesley Ott[y], Benjamin Poulter[z], Muye Ru[aa], Stanley P. Sander[b], Neil Swart[p], Yuk L. Yung[a,b], Zhao-Cheng Zeng[bb], and the rest of the Keck Institute for Space Studies "COVID-19: Identifying Unique Opportunities for Earth System Science" study team[1]

[a]Division of Geological and Planetary Sciences, California Institute of Technology; [b]Jet Propulsion Laboratory, California Institute of Technology; [c]Division of Engineering and Applied Science, California Institute of Technology; [d]Department of Chemical and Environmental Engineering, Center for Environmental Research and Technology, University of California, Riverside, CA 92521, United States; [e]Universities Space Research Association, Columbia, MD 21046, United States; [f]NASA Goddard Space Flight Center, Greenbelt, MD 20771, United States; [g]California Energy Commission, Sacramento, CA 95814, United States; [h]Department of Earth and Planetary Science, University of California, Berkeley, Berkeley, CA 94720, USA; [i]Department of Mechanical Engineering, University of Colorado at Boulder, Boulder, CO 80309 United States; [j]Department of Climate and Space Sciences and Engineering, University of Michigan, Ann Arbor, Michigan 48109, United States; [k]Department of Earth System Science, Tsinghua University, Beijing 100084, China; [l]Department of Atmospheric Sciences, University of Washington, Seattle, WA 98195, United States; [m]Milken Institute School of Public Health, George Washington University, Washington, DC 20052, United States; [n]Modeling and Meteorology Branch, California Air Resources Board, Sacramento, CA 95814, United States; [o]Department of Chemistry, University of Colorado Boulder, Boulder, CO 80309, USA; [p]Canadian Centre for Climate Modelling and Analysis, Environment and Climate Change Canada, Victoria, BC, Canada; [q]School of Informatics, Computing and Cyber Systems, Northern Arizona University, Flagstaff, AZ 86011, United States; [r]Science and Technology Advancement Division, South Coast Air Quality Management District, Diamond Bar, CA, 91765, USA; [s]Department of Environmental Sciences, University of California, Riverside, California, USA; [t]Center for Environmental Research and Technology, Riverside, CA 92521, United States; [u]Department of Physics, University of Toronto, Toronto, Ontario, Canada; [v]Department of Atmospheric and Oceanic Sciences and Institute of Arctic and Alpine Research, University of Colorado, Boulder, CO, USA; [w]McKelvey School of Engineering, Washington University in St. Louis, St. Louis, Missouri 63130, United States; [x]Department of Earth and Environmental Sciences, Columbia University, Lamont Doherty Earth Observatory, Palisades, NY 10964, United States; [y]Global Modeling and Assimilation Office, NASA Goddard Space Flight Center, Greenbelt, MD, United States; [z]Biospheric Sciences Laboratory, NASA GSFC Goddard Space Flight Center, MD, United States; [aa]The Earth Institute, Columbia University, New York, NY 10025, United States; [bb]Joint Institute for Regional Earth System Science and Engineering, University of California, Los Angeles, CA 90095, United States; [cc]Cooperative Institute for Research in Environmental Sciences, University of Colorado Boulder, Boulder, CO 80309, USA

The COVID-19 global pandemic and associated government lockdowns dramatically altered human activity, providing a window into how changes in individual behavior, enacted *en masse*, impact atmospheric composition. The resulting reductions in anthropogenic activity represent an unprecedented event that yields a glimpse into a future where emissions to the atmosphere are reduced. While air pollutants and greenhouse gases share many common anthropogenic sources, there is a sharp difference in the response of their atmospheric concentrations to COVID-19 emissions changes due in large part to their different lifetimes. Here, we discuss two key takeaways from modeling and observational studies. First, despite dramatic declines in mobility and associated vehicular emissions, the atmospheric growth rates of greenhouse gases were not slowed. Second, it demonstrated empirically that the response of atmospheric composition to emissions changes is heavily modulated by factors including carbon cycle feedbacks to CH_4 and CO_2, background pollutant levels, the timing and location of emissions changes, and climate feedbacks on air quality.

COVID-19 | air quality | greenhouse gases | Earth system | mitigation

The effects of the COVID-19 pandemic and associated lockdown measures have provided a way to observationally test predictions of future atmospheric composition. This is illustrated conceptually in Figure 1. With many people working from home and limiting travel, the pandemic caused a significant decrease in anthropogenic emissions. These emissions reductions can be thought of as a jump forward in time to a future where additional systemic emissions controls have been adopted. However, because these changes occurred in a matter of months, the changes to the concentrations of key air quality (AQ) and climate relevant gases in the atmosphere were readily observable. Combining these observations with current state-of-science models allows us an important window into the underlying processes governing the response of the Earth system to reductions in anthropogenic emissions, and thus a preview of the relative effectiveness of different emissions control strategies.

Our goal is to synthesize some of the key results from the past year into a coherent understanding of what we have learned about the effectiveness of different strategies to reduce greenhouse gas (GHG) emissions and improve AQ. We will do so in four parts. First, we summarize the observed changes

Significance Statement

The COVID-19 pandemic and associated lockdowns caused significant changes to human activity that temporarily altered our imprint on the atmosphere, providing a brief glimpse of potential future changes in atmospheric composition. This event showed key differences in how air quality and atmospheric greenhouse gas concentrations respond to changes in anthropogenic emissions, with implications for future mitigation strategies.

JLL led the manuscript and the human activity analysis. JN, DS, and POW led the study team. K. Barsanti, K. Bowman, DS, AT, and EK led study subgroups. Remaining authors contributed data analysis. All authors helped revise the manuscript.

The authors declare no competing interests.

[1]To whom correspondence should be addressed. E-mail: jlaugh@caltech.edu, jessica.l.neu@jpl.nasa.gov, david.schimel@jpl.nasa.gov, or wennberg@gps.caltech.edu

www.pnas.org/cgi/doi/10.1073/pnas.XXXXXXXXXX

PNAS | July 13, 2021 | vol. XXX | no. XX | 1–11
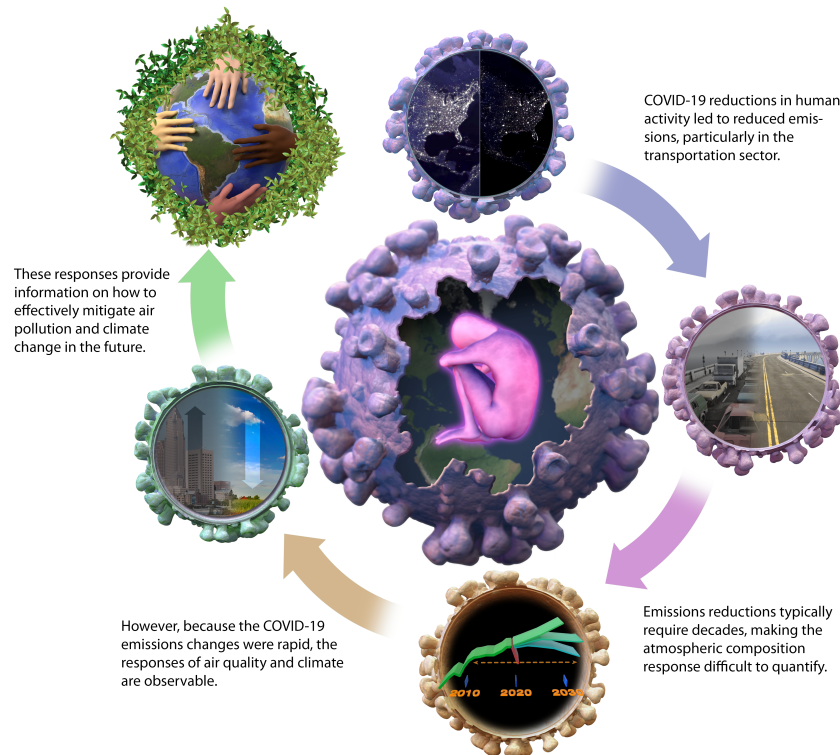
Fig. 1. Illustration of the conceptual foundation for this study. The COVID-19-induced reductions in human activity led to reduced anthropogenic emissions. The fact that these reductions occurred over months rather than decades allows us to observe how the atmosphere, land, and ocean are likely to respond in a future scenario with stricter emissions controls. This analysis helps to identify effective pathways to mitigate air pollution and climate change. Image credit: Chuck Carter / Keck Institute for Space Studies

in anthropogenic emissions during 2020. Second, we examine how the reduction in CO_2 emissions impacted the atmospheric CO_2 growth rate. Third, we show that the response of AQ to emissions reductions is very spatially heterogeneous, and summarize the causes of that heterogeneity. Fourth, we discuss the implications of these results for future AQ improvement strategies, our understanding of processes controlling GHG concentrations in the atmosphere, feedbacks between AQ, GHGs, and climate, and finally close by identifying strengths and gaps in our current observing networks. We draw three primary conclusions from this synthesis:

1. Despite drastic reductions in mobility and resulting vehicular emissions during 2020, the growth rates of GHGs in the atmosphere were not slowed.

2. The lack of clear declines in the atmospheric growth rates of CO_2 and CH_4, despite large reductions in human activity, reflect carbon cycle feedbacks in air-sea carbon exchange, large interannual variability in the land carbon sink, and the chemical lifetime of CH_4. These feedbacks foreshadow similar challenges to intentional mitigation.

3. The response of AQ to emissions changes is heavily modulated by factors including background pollutant levels, the timing and location of emissions changes, and climate-related factors like heat waves and wildfires. Achieving robust improvements to AQ thus require sustained reductions of both AQ and GHG emissions.

Summary of emissions in 2020

As AQ-relevant gases and CO_2 are co-emitted by combustion processes, decreases in human activity are expected to drive decreases in both of these species. Figure 2 summarizes changes to key sectors of human activity during the COVID-19 pandemic. Figure 2a shows the Oxford Stringency Index (1), which quantifies the severity of government-imposed restrictions on travel, businesses, schools, and other aspects of society. Panels b, c, and d show changes in air travel & maritime shipping, traffic, and United States (US) electricity use, respectively. There is a clear decrease in air travel and traffic for most of the world in March 2020, when the first major wave of COVID-19 led governments to institute quarantine measures (see also high values of the Stringency Index). Maritime shipping (to west coast US ports) and power generation (in the US) were less affected. Power generation in particular remained within approximately 5% of 2019 levels.

Reductions in NO_x emissions were apparent in both in situ (5) and satellite (6) observations of NO_2 concentrations due to the short atmospheric lifetime of NO_x (< 1 day). Estimates of NO_x emissions reductions from assimilating satellite data in global models (7), combining global chemical models with machine learning trained on surface measurements (8), or activity data (including electricity use, traffic/mobility data, flight data, etc.) (9–11) find regional reductions of 10% to 40% during the strictest lockdown periods. Generally, methods assimilating satellite data report smaller reductions (10% to 20%) than studies based on activity data (25% to 40%).
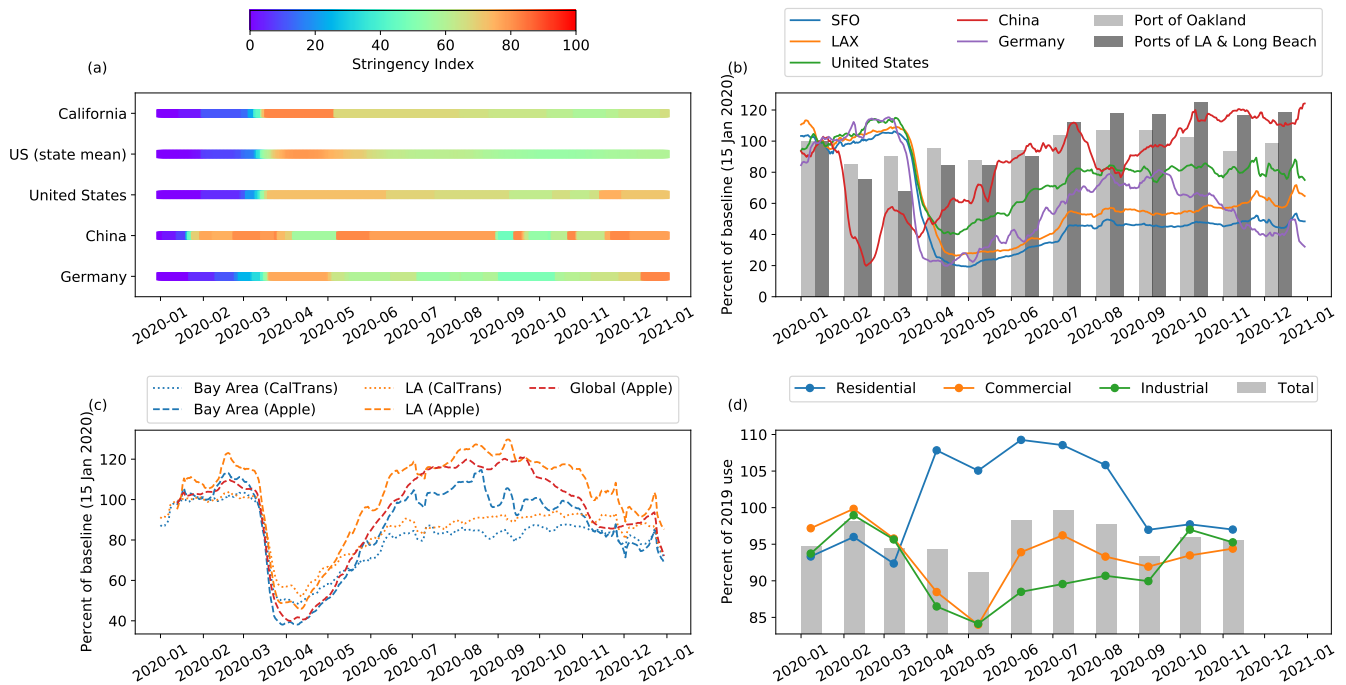
Fig. 2. Metrics for change in human activity at different scales show that the strongest impact of COVID-19 lockdowns were in the transportation sections, and that these impacts varied substantially from country to country. Panel **(a)** shows the Oxford stringency index (1) for the regions used in this figure. "US (state mean)" is the average of individual states' indices, "United States" is the index attributed to the US as a whole (not individual states, see SI for discussion). Panel **(b)** shows the percent change in flights (2–4) for two California airports and three countries (lines) and container moves for three California ports (bars) Panel **(c)** shows traffic metrics for two California urban areas, and 26 countries ("global"). CalTrans indicates Caltrans PEMS data; Apple indicates Apple driving mobility data. Panel **(d)** shows electricity consumption in the US by sector, relative to the same month in 2019. The three sectors shown constitute $> 96\%$ of US power consumption. In **(b)** and **(c)**, daily metrics are relative to 15 Jan 2020 and presented as 7 day rolling averages and monthly metrics are relative to Jan 2020. Electricity consumption not available after Nov 2020 at time of writing.
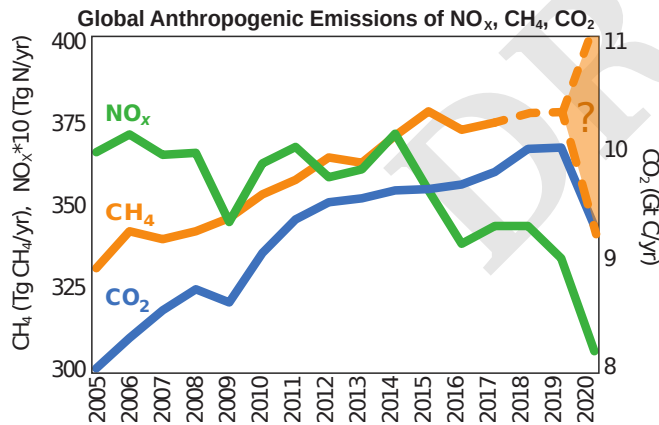
Fig. 3. 2020 saw reductions in CO_2, CH_4, and NO_x emissions. CH_4 and NO_x are plotted along the left axis, CO_2 on the right. The dashed line for CH_4 after 2017 indicates it is estimated from the average rate of increase. 2020 emissions are represented as a range: the IEA estimated a 10% decrease in CH_4 emissions in 2020(12), but this is uncertain, as the CH_4 growth rate increased in 2020. Full details are in the SI.

Estimates of the reduction in global NO_x emissions in the first half of 2020 range from 5% (8) to 13% (7).

The change in global CO_2 emissions was comparable to that of NO_x emissions, as seen in Fig. 3. Liu et al. report a peak global reduction of approximately 15% (4 Tg C or 15 Mt CO_2) in April, and an annual total of 5.4% (13). In March 2020, Le Quéré et al. projected a slightly larger 7%
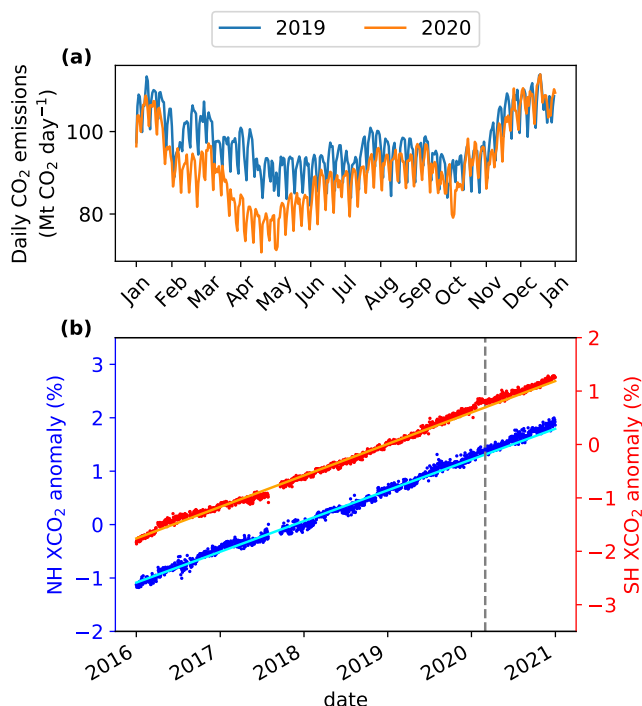
decrease in CO_2 over the remainder of 2020 (14). The largest decreases occurred in the first half of 2020, as shown in Fig. 4a and were primarily associated with reductions in ground transportation (15). The response of atmospheric CO_2 mixing ratios can be observed near the emissions sources; during the strictest lockdowns, Turner et al. were able to use CO_2 observations from a local ground-based network to estimate a 48% reduction in traffic CO_2 emissions in the San Francisco Bay Area (16). Liu et al. found a 63% (41 ppm) decrease of the typical on-road CO_2 enhancement in Beijing, China (17). Distinguishing these signals in CO_2 at regional scales is more challenging. Buchwitz et al. infer peak decreases in anthropogenic CO_2 emissions from China of 10% from space-based total column CO_2 measurements (18). However, they note that the uncertainty is approximately 100%, and that the expected CO_2 concentration signal is 0.1 to 0.2 ppm, out of a background of over 400 ppm.

Anthropogenic CH_4 emissions are dominated by sources such as landfills, oil and gas production, and agricultural activities. The International Energy Agency (IEA) estimates that CH_4 emissions dropped by 10% in 2020 (Fig. 3), largely due to the decrease in demand for oil and gas. However, it is unclear whether reduced demand during 2020 was the primary driver of emissions. It is likely that decreased maintenance of landfills and oil and gas infrastructure during the COVID-19 pandemic led to new leaks in some areas, which can result in those locations becoming CH_4 "superemitters" (19). In general, the type, maintenance level, and throughput of CH_4 infrastructure can have a large impact of the amount of fugitive

Fig. 4. Despite substantial reductions in anthropogenic CO_2 emissions in early 2020, the annual atmospheric CO_2 growth rate did not decline. Panel **(a)** shows daily global CO_2 emissions for 2019 and 2020, calculated following Liu et al. (13). Panel **(b)** shows trends in atmospheric column average CO_2 from the Orbiting Carbon Observatory 2 (OCO-2). The small blue and red symbols indicate daily, deseasonalized values as percent anomalies relative to the global 2018 mean. The solid cyan and orange lines are linear fits to 2016 through 2019 data. In panel (b) the vertical gray dashed line marks 1 March 2020 as the approximate beginning of lockdowns in response to COVID-19. A version of (b) showing the absolute trends and the data including the seasonal cycle is available as Fig. S8 in the SI.

113 emissions (20, 21). On a positive note, some of the decrease
114 in emissions estimated by the IEA was associated with the
115 installation of new oil and gas infrastructure and the adoption
116 of new CH_4 regulations in a number of countries (12). Such
117 decreases would likely be sustained beyond the pandemic
118 period.

CO_2 and CH_4 atmospheric growth rates

120 The effect of CO_2 emissions reductions, especially from ground
121 transport, were clearly apparent in urban-scale observations
122 of atmospheric CO_2 mixing ratios (16, 17). This does not,
123 however, transfer to global-scale observations. Figure 4b shows
124 deseasonalized trends in column-average CO_2 mixing ratios
125 (referred to as XCO_2) observed by the Orbiting Carbon Ob-
126 servatory 2 (OCO-2) instrument. Despite the reduction in
127 CO_2 emissions in 2020 (Fig. 4a), there is no clear deflection of
128 the observed XCO_2 below what would be projected based on
129 previous years' growth rates. We compared the variability in
130 actual atmospheric CO_2 growth rates derived from the OCO-
131 2 data with that computed from fossil fuel emissions (Fig.
132 S8b) and found that the change in atmospheric CO_2 growth
133 caused by the COVID-19 pandemic is smaller than the natural
134 year-to-year variability. This is expected, because the percent
135 change in the CO_2 growth rate, in the absence of feedbacks,
136 will match the percent change in emissions. For a typical
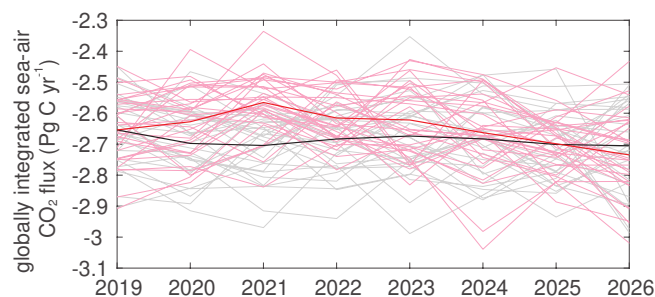
Fig. 5. Sea-air carbon exchange responded quickly to the reduction in anthropogenic CO_2 emissions during 2020. Shown here are annual mean, globally integrated sea-to-air carbon dioxide fluxes predicted from the CanESM5-COVID ensemble (24, 25). Black/gray lines derive from simulations forced with SSP2-RCP4.5 CO_2 emissions, while red/pink lines derive from simulations forced with a 25% peak CO_2 emissions reduction in 2020. See (24, 25) for more details. Thick lines are ensemble averages, and thin lines are individual ensemble members, each with different phasing of internal variability.

137 growth rate of 2.45 ppm/year since 2016 (Fig. S8b and 22),
138 the 5.4% total reduction in CO_2 emissions calculated by Liu
139 et al. (13) equals a 0.13 ppm/yr decrease in the CO_2 growth
140 rate for 2020—well within the natural variability observed by
141 OCO-2 (Fig. S8) and surface networks (22).

142 Wildfires are one element of the variability in CO_2 growth
143 rate. The 2019/2020 Australian wildfires emitted 173 Tg C
144 (634 Mt CO_2) between Nov 2019 and Jan 2020, over 6 times
145 more than Australia's average Nov.-Jan. CO_2 emissions for
146 2001 through 2018 (23). This drove an early increase in CO_2 in
147 2020, evident in the deseasonalized southern hemisphere OCO-
148 2 XCO_2 (Fig. 4b, red series) and growth rate derived from the
149 OCO-2 data (Fig. S8b). This wildfire anomaly offset a third
150 of the 518 Tg C (1901 Mt CO_2) reduction in anthropogenic
151 CO_2 (13) and so does not fully explain the offset between
152 emissions and atmospheric mixing ratios for CO_2.

153 The atmospheric CO_2 growth rate led to a reduction in the
154 rate of oceanic CO_2 uptake. Figure 5 shows the magnitude of
155 ocean carbon fluxes over 8 years as computed from a model
156 ensemble under normal and COVID-like emissions. There is
157 significant variation in the sea-air and CO_2 flux among the
158 model ensemble members. This spread represents the potential
159 interannual variability in CO_2 flux; given that variability, the
160 true change in CO_2 flux in 2020 is uncertain, in part due to
161 corresponding variability in the land carbon sink (Fig. S9).
162 However, the ensemble mean indicates that while on short
163 time scales the land carbon flux is insensitive to the change
164 in emissions (Fig. S9), the ensemble mean ocean uptake was
165 reduced by 70 Tg C/yr in 2020. This would offset 14% of the
166 approximately 520 Tg C/yr (1901 Mt CO_2/yr) reduction in
167 anthropogenic CO_2 emissions in 2020 (13), further dampening
168 the signal from emissions reductions in atmospheric CO_2.

169 The growth rate of CH_4 was also not slowed by the pan-
170 demic. Figure 6a shows trends in column average CH_4 (XCH_4)
171 from two ground based spectrometers in the Total Carbon
172 Column Observing Network (TCCON, 26, 27) located in Park
173 Falls, Wisconsin, US (28) and Lauder, New Zealand (29, 30).
174 The XCH_4 values after 1 March 2020 lie approximately 0.3%
175 above the 2016 to 2019 trend in both hemispheres. Similarly,
176 NOAA reported the single largest increase in CH_4 in its record
177 (31).

178 Because the lifetime of CH_4 depends on the abundance of

(a)

(b)
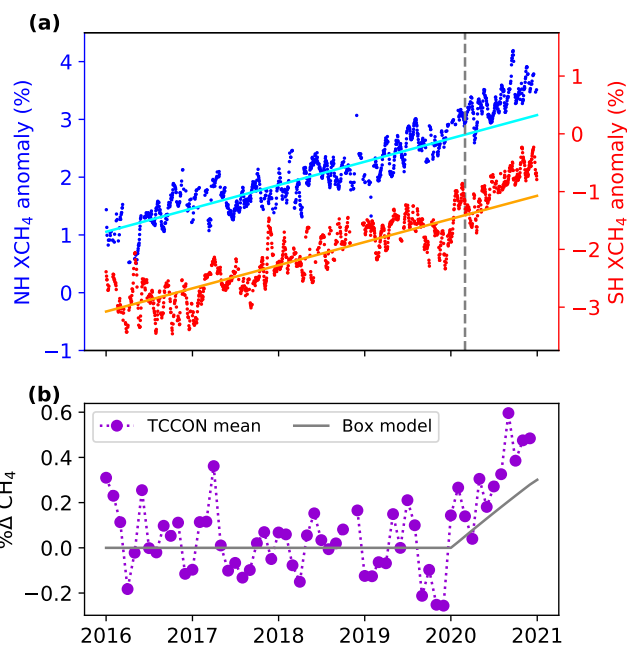
Fig. 6. Atmospheric mixing ratios of CH_4 increased more rapidly in 2020 than they had in the past decade. The increase is consistent with no change in CH_4 emissions and a 3% decrease in OH (predicted from decreased NO_x emissions) during 2020. Panel **(a)** is similar to Fig. 4b, except it shows trends in column-average CH_4 (XCH_4) from two TCCON sites: Park Falls, WI, USA in the northern hemisphere and Lauder, New Zealand in the southern hemisphere instead of OCO-2 XCO_2. Panel **(b)** compares the TCCON XCH_4 trend to that predicted by a box model. The purple series are the monthly mean percent differences between the TCCON XCH_4 and linear fits from (a). The grey line represents the percent difference in CH_4 predicted by a box model (33) with a 3% decrease in OH during 2020 compared to no change in 2020 OH.

the hydroxyl radical (OH), the concentration of CH_4 varies with atmospheric pollution levels. In fact, we find compelling evidence that the jump in CH_4 mixing ratios during 2020 is partly due to reductions in NO_x emissions. In a model incorporating the decreased NO_x emissions associated with COVID-19 (32), the resulting decrease in global ozone (7) leads to a 2% to 4% decrease in global OH concentrations. As oxidation by OH is the primary loss process for atmospheric CH_4, this acts to increase CH_4 mixing ratios in the atmosphere. Figure 6b compares the trend in XCH_4 measured by TCCON to that predicted by a box model (33). The purple series is the monthly percent difference of TCCON XCH_4 from the linear trends shown in Fig. 6a, and the gray line is the percent difference between a box model run with and without a 3% decrease in OH during 2020. The box model closely matches the extra growth in atmospheric CH_4 during 2020, indicating that the change in OH was an important driver of the observed CH_4 growth. However, this is inconsistent with the 10% decrease estimated by the IEA (12), as our box model assumes constant CH_4 emissions after 2012.

If decreases in anthropogenic NO_x emissions during 2020 were responsible for the increase in CH_4 lifetime that led to its higher than expected growth rate, what does this imply for the effect of future efforts to reduce NO_x emissions to improve AQ? To understand this, we need to examine how the 2020 NO_x decreases affected AQ around the world. In the next section, we will describe the ozone and particulate matter (PM) response to these NO_x reductions. Afterward, we will explore the implications of this AQ-GHG in the discussion.

Heterogeneity in air quality response

Most parts of the world saw significant decreases in NO_x emissions during the pandemic, but the magnitude and timing of these emissions changes varied with location. Figures 7a-c compare timeseries of NO_2 column densities measured by TROPOMI for three cities. Following the beginning of lockdown measures (indicated by the dotted lines), the 2020 NO_2 column densities are clearly less than in 2019. However, in Los Angeles, the drop in NO_2 occurred very rapidly when lockdowns were enacted in early March, but by May there was little difference between 2019 and 2020. In Lima, on the other hand, the difference between 2019 and 2020 grew from March through May. In Shanghai, we see a very large drop in NO_2 associated with the early lockdown in January and a smaller drop during the second lockdown in late February.

These changes in NO_x emissions drove changes in secondary pollutants, such as ozone and PM. However, the ozone and PM responses depended on the local chemical regime and meteorology, as well as the magnitude and timing of the NO_x emissions reductions. In this section, we describe the factors controlling the ozone response first, followed by PM.

Ozone. Ozone is a secondary pollutant produced in the atmosphere from the reaction of NO_x and OH with volatile organic compounds (VOCs). The response of ozone concentrations to changes in NO_x emissions is characterized by the ozone production efficiency (OPE), which is the ratio of the change in ozone for a given change in NO_x.

Figures 7d-f show the ozone production efficiency (OPE) calculated in a global model that assimilates multiple satellite measurements. The OPE values shown represent the change in ozone mass burden per unit change in mass of reactive nitrogen emissions, using the COVID-19 reduction in emissions as the ΔNO_x. More detail is given in the SI.

Two patterns in the OPEs demonstrate the significant spatial and temporal variability in the relationship between NO_x emissions and ozone concentrations. First, in Fig. 7f, the OPE in the Northern hemisphere increases between February and June. This is mostly due to increasing sunlight driving key photolysis reactions more rapidly. Thus, the timing of NO_x emissions changes plays a significant role in the magnitude of the ozone response in the mid- and high-latitudes, with a smaller ozone response to a given NO_x change during spring than during summer. Second, in Fig. 7d, tropical and subtropical cities have the largest, most positive OPEs. Furthermore, there is little change in OPE with season for these cities (Fig. 7e) due to the relatively small changes in insolation at low latitudes. Figure 7d indicates that most of the northern mid-latitude cities have small, positive OPEs. Two cities, however, have slightly negative OPEs (Beijing -0.10, Karachi -0.06); a negative OPE indicates that ozone increased when NO_x emissions decreased. Other studies have, in fact, identified large ozone increases in China (34) associated with the decreased NO_x emissions during the pandemic. Additional increases in ozone were observed in Europe (35), with smaller but still positive changes in ozone in the United Kingdom (36).

We use a steady-state model (Fig. S10) to interpret the patterns in Fig. 7. From the steady-state model, we know OPE is small at both low and high NO_x concentrations, but large at

Laughner *et al.*

PNAS | **July 13, 2021** | vol. XXX | no. XX | **5**
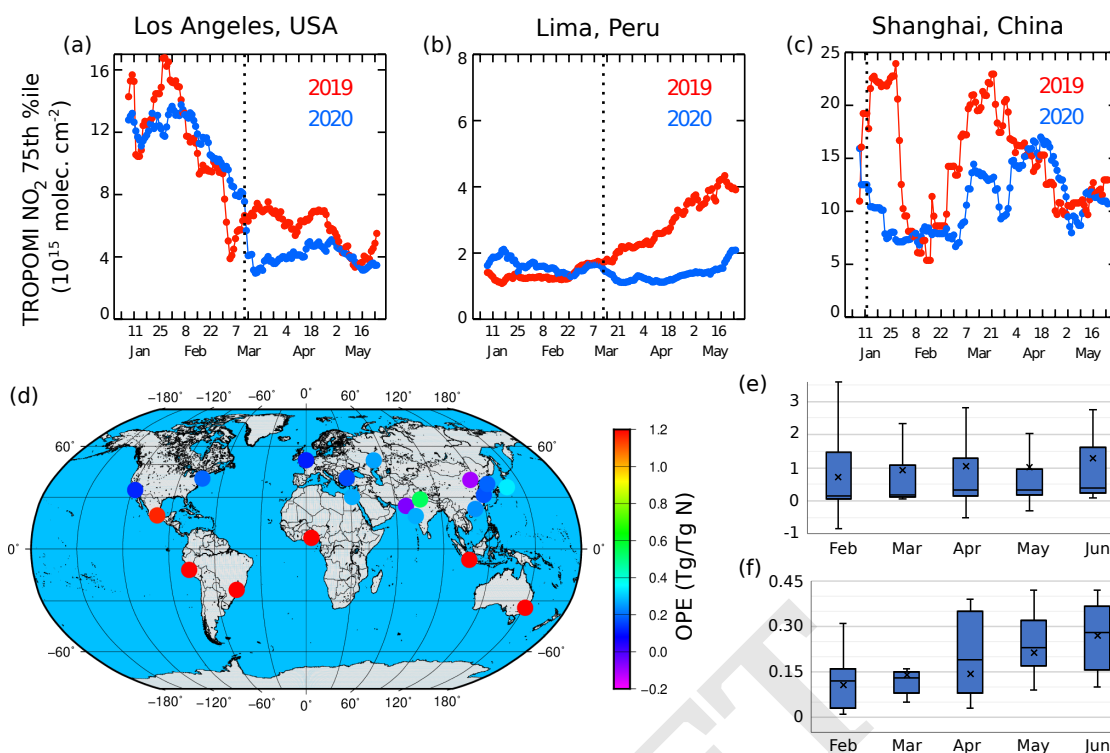
Fig. 7. COVID-19 lockdowns dramatically reduced urban NO$_2$ levels, which in turn drove changes in O$_3$ production. Panels **(a–c)** show 15 day rolling averages of 75th percentile TROPOMI NO$_2$ column densities in three cities for 2019 and 2020. The vertical dotted line indicates the beginning of lockdown measures in 2020. Panel **(d)** shows OPE modeled in 17 megacities, averaged from February to June 2020. Panel **(e)** shows modeled monthly global averaged tropospheric O$_3$ production efficiency (OPE). The whiskers are the minimum and maximum, the horizontal lines the quartiles and median, and the X is the mean. Panel **(f)** is similar to (e), but averaged over 30° N to 90° N.

intermediate NO$_x$ concentrations. Overall OPE also increases with VOC reactivity (VOC$_R$, the total rate of reaction of all VOCs with OH in a given parcel of air) for NO$_x$ concentrations greater than ~ 0.1 ppb. Thus, in Fig. 7, areas with negative OPE are in the high-NO$_x$ part of the OPE curve; sustained efforts to reduce NO$_x$ emissions will bring them closer to the maximum-OPE tipping point, after which NO$_x$ reductions should lead to ozone reductions. Cities in the tropics and subtropics have large, positive OPE values. This is partly due to plentiful sunlight to drive photochemistry, but these regions also have large VOC$_R$ values due to the abundance of biogenic VOCs (37). The steep dependence of OPE on NO$_x$ follows because NO$_x$ is the limiting reactant in ozone production in these high-VOC$_R$ conditions. Thus, these cities should see large ozone reductions from NO$_x$ reductions. However, of the equatorial cities shown in Figure 6, only those located in South Asia had large enough reductions in NO$_x$ emissions during the COVID-19 pandemic to produce substantial reductions in surface ozone (3-5 ppb) (7).

We also see this heterogeneity in ozone response to NO$_x$ emissions reductions at the intraurban scale. Measurements of daily maximum NO$_2$ and ozone at monitoring sites throughout the Los Angeles Basin show consistent reductions in NO$_2$ throughout the basin in March and April of 2020, but smaller reductions in ozone in the central northern part of the basin than elsewhere (Figs. S1, S2). This is consistent with the near-0 OPE for Los Angeles in Fig. 7d, i.e. for a city on the verge of reducing NO$_x$ emissions to the point where NO$_x$ is the limiting factor in ozone production. While the overall basin chemistry is at this tipping point, local differences in emissions

as well as transport of pollutants within the basin can lead to these small scale differences in ozone response (38).

However, the behavior of ozone in the Los Angeles Basin also illustrates that NO$_x$ controls may become less effective in a warmer climate. Figure 8 shows time series of daily maximum NO$_2$ and ozone (top and middle panels). NO$_2$ and ozone concentrations are clearly lower in March and April 2020 compared to the 2015 to 2019 average, in part due to the reduction in NO$_x$ emissions at the beginning of the lockdown. However, these two months were significantly cooler than the 2015 to 2019 average as well. When temperatures rose above average during an unusual heat wave in late April and May of 2020, ozone daily maxima rose above the range seen in 2015 to 2019, despite the fact that NO$_2$ remained similar to 2015 to 2019 concentrations. An increase in ozone during April and May was also seen in a previous study (39). The response of ozone per degree increase in temperature is shown in Fig. S3. Typical values for the O$_3$ season (May-Sep) in 2020 throughout the basin were 1.8 to 5.8 ppb K^{-1}. This is higher than a previous prediction of about 1 ppb K^{-1} in the basin (40), suggesting the ozone climate penalty may be stronger than expected; however, analysis is ongoing.

Particulate matter. Achieving long-term reductions in PM (especially PM 2.5, particles with a diameter $< 2.5 \mu$m) concentrations is a matter of great importance due to the large health impacts of PM compared to ozone (41). Our interest here is to use observations from the pandemic period to better understand some of the factors controlling atmospheric PM concentrations, rather than focusing on the question of whether
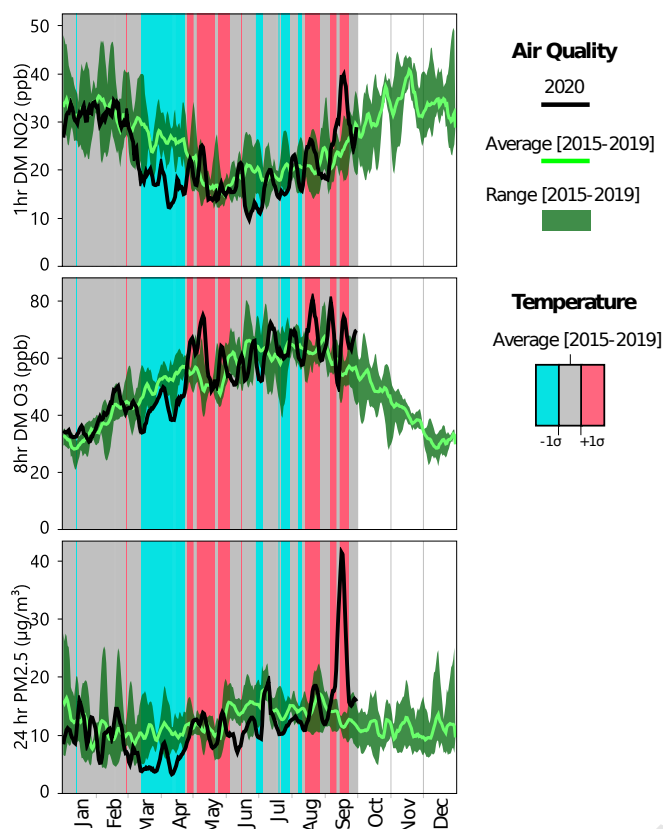
Fig. 8. In Los Angeles, temperature and wildfires drove ozone and PM pollution, respectively, more than changes in traffic. The three panels show 7-day rolling average of 24hr PM$_{2.5}$, 1hr daily maximum (DM) NO$_2$, and 8hr DM O$_3$, respectively, by day of year in 2020 and in the past five years (2015-2019) in the LA Basin. Bars in the background show the 7-day rolling average of basin-average 1 hr DM temperature in 2020 relative to the 2015 to 2019 average ($\pm 1\sigma$) by day of year. 2020 data are preliminary, unvalidated, and subject to change.

PM exposure increases the chance of death from COVID-19.

The factors controlling PM concentration are more complicated than those for ozone. PM arises from primary emissions and natural sources, as well as secondary chemistry in the atmosphere. One such secondary pathway is the formation of nitrate PM from the reaction of higher oxides of nitrogen (such as HNO$_3$) with ammonia (42). Nitrate PM formation via this pathway may be limited by either available NO$_x$ or ammonia.

Model simulations (Fig. S4) demonstrate the effect that NO$_x$ emissions reductions had on nitrate PM formation in Los Angeles. Under COVID-19 emissions, the nitrate PM concentrations decreased by approximately 60% in April 2020. At the same time, the model reported a shift towards NO$_x$-limited (rather than ammonia-limited) chemistry. This implies that the NO$_x$ emissions decreases in April, when the shift in the chemical regime shows the largest change, were more efficient at reducing nitrate than the reductions in other months. Compared to the measured total PM reductions shown in the bottom panel of Fig. 8, our results suggest that NO$_x$ emissions reductions account for about 10% of the total PM reduction in the Los Angeles Basin during the COVID-19 lockdowns. This agrees with other recent work (43) which indicate that traffic NO$_x$ emissions contribute less than 10% of secondary

PM production throughout North America, Europe, and East Asia.

The relative availability of NO$_x$ and ammonia elsewhere in the US plays an important role in whether NO$_x$ emissions reductions lead to reduced nitrate PM. Simulations of nitrate chemistry over the continental US show that Los Angeles is somewhat unique as an urban area that experienced a significant shift to NO$_x$-limited nitrate chemistry. Other urban areas in the northeast, southeast, and northwest largely remained ammonia-limited (Figs. S5–S7). This could explain, at least in part, the scattered response of PM to NO$_x$ emissions reductions across US cities seen in other studies (44). It also implies that continuing the long-running trajectory of NO$_x$ emissions reductions in Los Angeles in order to reach the tipping point where ozone becomes NO$_x$ limited will also benefit AQ via reduced production of nitrate PM.

However, Los Angeles also represents a cautionary tale about attributing AQ changes to the COVID-19 pandemic without accounting for other confounding factors. Weather and wildfires also played a large role in determining the PM concentrations in Los Angeles during 2020. When the lockdowns were first instituted in March, news outlets and social media attributed the clean air in the Los Angeles Basin to the lack of traffic. However, as seen in Fig. 8, the lower PM concentrations in March and April 2020 than 2015 to 2019 (Fig. 8, bottom) coincide with anomalously cool weather, which was accompanied by higher than average precipitation (Fig. S1 in (38)). Precipitation removes PM from the atmosphere through wet deposition (45, 46), and was at least partially responsible for the clean air during this period. The extreme spike in PM concentrations seen in September 2020, on the other hand, coincides with a time period when major wildfires were burning in close proximity to Los Angeles. Like the April-May heatwave, this event also points to the fact that climate change can erase progress in AQ improvement through emissions reductions.

Discussion

The changes in atmospheric composition throughout 2020 unequivocally demonstrate that AQ and GHGs cannot be treated as separate problems, despite the disparate time scales of AQ and GHG responses to changes in human activity. AQ is most dependent on local changes in emissions because of the shorter atmospheric lifetime and rapid chemistry of AQ-relevant pollutants. In contrast, the global total GHG emissions matter more than local emissions, as it is the overall GHG atmospheric growth rate that drives climate change. As discussed above, improvements in AQ made by reducing pollutant emissions locally can be offset by changes in meteorology or non-anthropogenic (e.g. biogenic or wildfire) emissions driven by climate change. Likewise, changes in AQ can affect climate change, as decreases in AQ-relevant emissions could lead to increased lifetimes for shorter-lived GHGs (such as CH$_4$), increasing their global warming potential.

Reductions in NO$_x$ emissions during the pandemic did show the potential benefits cities can gain by promoting systemic change to accomplish these same reductions. For most countries, the pandemic-induced emissions reductions can be seen as going back in time to a period when NO$_x$ emissions were lower. In the US, Europe, and China, where NO$_x$ emissions have been trending downward, these reductions were more

COVID-19 Equivalent NOₓ Emissions Year by Country

2005 2007 2009 2011 2013 2015 2017 2019 2021 2023 2025 2027 2029
[year]
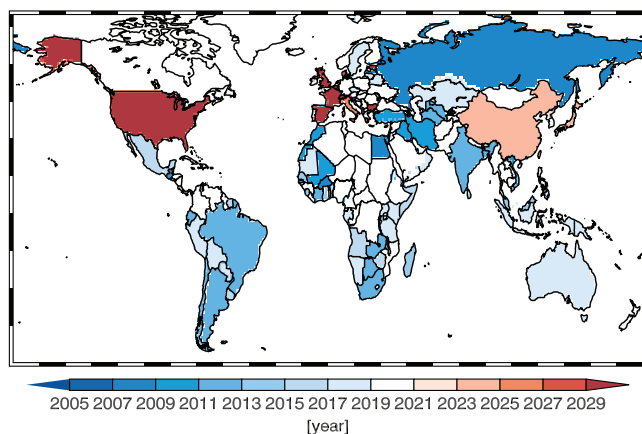
Fig. 9. The emissions reductions during the pandemic are, in a sense, like moving forward or back in time. Countries are colored by the year to which their 2020 NO_x emissions are equivalent, projected forward in time where emissions have been decreasing and backward elsewhere. Details of emissions estimates given in the SI.

akin to a jump forward in time to a lower emissions future. Figure 9 shows the equivalent year for each country's NO_x emissions during the pandemic, assuming recent trends in NO_x emissions hold constant. Most striking is how much more quickly China could reach pandemic-like emissions levels than the US or Europe. Though all three regions' emissions reductions had similar peak magnitudes (18% to 20%), Europe and especially the US are further along their respective NO_x reduction pathways than China. This, combined with China's higher pre-pandemic emissions levels, means that China can make progress quickly if they are able to maintain the aggressive pace of emissions reductions they have set over the past decade (32).

Many cities in the US and Europe are close to reaching a point at which NO_x emissions will be a very effective control on ozone concentrations. In Fig. 7d, cities with an OPE near 0 are likely at the tipping point between VOC-limited and NO_x-limited chemistry. Further NO_x reductions should move them firmly into NO_x-limited chemistry, where NO_x is the primary control on ozone formation. While sustaining these emissions reductions may be challenging due to the decreasing contribution of on-road gasoline emissions (47) and the impact of emissions reductions being offset in part by increases in chemical lifetime (48), the rewards in doing so are likely substantial. In addition, since NO_x and CO_2 are co-emitted by combustion processes, regulations such as those that encourage a transition to electric vehicles will also benefit climate. In fact, recent work has shown that the cost savings associated with reduced health impacts from air pollution will outweigh the cost of transition to a clean carbon economy and that the increased radiative forcing from longer-lived CH_4 and ozone is balanced by the decrease in forcing from smaller CO_2 mixing ratios (49). On the other hand, measures such as NO_x removal from coal-fired power plants will benefit AQ but not climate; as discussed below, this will eventually limit their effectiveness for improving AQ.

The same strategies to improve AQ will not be equally effective in all locations. On one hand, the tropical and subtropical cities with large, positive OPE values in Fig. 7d can immediately realize substantial ozone reductions through reductions in NO_x emissions. On the other hand, cities such as Beijing and Karachi with negative OPEs, or locations such as the United Kingdom where in situ studies found a negative correlation between NO_x emissions and ozone concentrations (36) would do better to reduce volatile organic compound (VOC) reactivity simultaneously with NO_x emissions. Such an approach would allow them to avoid the chemical regimes with the largest OPEs (50) (Fig. S10a). Similarly, while chemical formation of ammonium nitrate PM in Los Angeles became NO_x-limited during the pandemic, most other cities in the US remain ammonia-limited and would see stronger reductions in PM by controlling primary emissions, organic precursors, or other key species.

Unfortunately, 2020 has also shown that improvements in AQ are likely to be offset by climate feedbacks. Such effects were most apparent in Los Angeles, where warmer than average May temperatures led to ozone concentrations above the 2015 to 2019 average, greater than average precipitation in March and April likely contributed to the reduction in PM, and severe wildfires from late August through September caused PM concentrations four times that of the 2015 to 2019 average. Changing climate will affect each of these variables, leading to warmer temperatures, more wildfires (51), and potentially more intense but less frequent precipitation (52), giving PM more time to accumulate between wet deposition events.

Changes in AQ-relevant emissions, particularly NO_x emissions, have potential to feed back into climate change as well. As we showed in Fig. 6, there is compelling evidence that reductions in OH stemming from reduced anthropogenic NO_x emissions drove a $\sim 0.3\%$ jump in CH_4 during 2020. While tropical cities have the greatest potential for decreasing ozone by reducing NO_x emissions (Fig. 7d), they also have an outsized impact on atmospheric CH_4 lifetime, as the largest share of CH_4 oxidation occurs in the tropics (33). Since only tropical cities in South Asia had substantial changes in NO_x emissions during 2020 (7), 2020 represents a minimum benchmark for the effect of NO_x reductions on the CH_4 growth rate. It is therefore essential to invest strategies to reduce fugitive CH_4 emissions (such as updated CH_4 storage and transportation infrastructure to prevent and limit leaks, landfill CH_4 capture, and confined animal feed operation CH_4 mitigation) ahead of decreases in tropical NO_x emissions.

In terms of climate, despite a reduction in global emissions equivalent to going back in time nine years (to 2011-equivalent CO_2 emissions), any change to the global CO_2 growth rate was smaller than typical interannual variability. As mentioned earlier and discussed in more detail below, this is partly due to the offsetting reduction in ocean carbon uptake (Fig. 5), but also arises because the sharp decreases in CO_2 emissions during the first half of 2020 were not sustained. By the second half of 2020, emissions due to power generation, industry, and residential consumption had nearly returned to 2019 levels (13). If we assume that these emissions levels represent a balance between reduced activity to limit the spread of COVID-19 and sufficient activity to maintain a minimum economic productivity, this suggests that reducing activity in these sectors is not practical. Reducing these sectors' emissions permanently will require their transition to low carbon emitting technologies.

One interesting aspect of the GHG emissions reductions during the pandemic was that they provided a chance to study

the feedback in ocean carbon uptake. The model simulations using COVID-like CO_2 emissions shown in Fig. 5 indicate that the sea-air carbon flux adjusts rapidly in response to changes in anthropogenic emissions. That model ensemble mean indicates a response time of about one year. Though this basic response - a decline of the ocean carbon sink in response to mitigation - is accounted for the RCP scenarios (53), much uncertainty remains as to the accuracy of these ocean sink predictions. This uncertainty is due both to the forced response of the ocean and to interannual variability Lovenduski et al. found that, for a change in ocean carbon uptake to be observable with our current network of ocean buoy measurements, it would need to be four times larger than the COVID-19 emissions reductions (25). This will be a challenge as we work to quantify the effect of future permanent CO_2 emissions reductions on atmospheric CO_2 mixing ratios.

The pandemic does offer insight into how the atmospheric GHG growth rates could be curtailed: systemic changes are required to enable sustained reductions in emissions. The efficacy of sustained reductions (without systemic changes to the energy sector) can be seen in the contrast between CO_2 emissions from ground transport and international shipping and aviation ("international bunkers") reported by Liu et al. (13) The peak reduction in international bunkers' emissions was only approximately 1/3rd that of the reduction in emissions from ground transport, by mass. However, while ground transport recovered fairly quickly, the international bunkers' emissions remained at about half of 2019 levels throughout the second half of 2020. As a result, the cumulative reduction in 2020 emission due to international bunkers was 75% that of the reduction due to traffic, despite the comparatively small magnitude of the daily emissions from international bunkers.

Sustained reduction in other sectors will require investment in renewable energy and new technologies to support current levels of productivity with lower carbon emissions, that is, to reduce the carbon intensity of our economy. Such investment is essential, as several studies (54, 55) have documented the harm to employment, family connections, and other critical human connections from the reduction in personal mobility due to the pandemic. Liu et al. (13) note that Spain's 2020 emissions due to power generation were almost 25% lower than in 2019 due to investment in renewable energy. A post-COVID economic recovery represents an opportunity to invest in carbon-reducing technologies (56), as long as the need to balance short-term job creation with long-term retraining is accounted for (57). If this investment was able to continue the trend of a 5.4% decrease in global CO_2 emissions per year, we would reach "preindustrial" (circa 1850) emissions levels in approximately 18 years.

Strengths and weaknesses of current observing systems

Understanding how the COVID-19 pandemic has altered AQ and the carbon cycle has relied heavily on the multifaceted observing system built over the past two decades, including satellites, dense ground-based observing networks, Earth system and chemical transport models, and techniques to assimilate observations into these models. Novel data on human activity (particularly internet-of-things mobility data, crowdsourced air traffic data, and even news reports) have also played a vital role in both understanding how human behavior changed during the pandemic and quantifying the effect of that change on anthropogenic emissions.

Nevertheless, there remain important gaps in our observing network. First, space-based detection of VOCs remains a challenging problem, yet quantitative measurements of key biogenic (e.g. isoprene, terpenes) and anthropogenic (e.g. ethene, propene) contributors to VOC OH reactivity are needed to identify the dominant chemistry governing AQ around the globe. Second, as we saw in the LA Basin case study, disentangling primary PM emission, secondary PM formation, and meteorological drivers of PM concentration is crucial to understand which processes control PM exposure. Given the serious health impacts of PM exposure, work towards an integrated surface and space-based system that can differentiate these processes is needed to elucidate the optimum approaches to reducing PM exposure.

In regards to climate-relevant observations, spatiotemporally broader and denser space-based GHG observations would provide a highly valuable empirical constraint on changes to anthropogenic and biogenic carbon fluxes. A satellite instrument that provided comparable observations to the $BEACO_2N$ network in the San Francisco Bay area ($\sim$ 2 km resolution, strong sensitivity to the near-surface atmosphere, urban-scale coverage) could apply similar inversion techniques as Turner et al. (16) to infer key sectors' emissions in cities around the world. It is also clear that our current network of near-real time ocean carbon uptake measurements are not sufficient to disentangle internal variability in the air-sea carbon flux from changes driven by reductions in anthropogenic emissions (25). Expanding this network or developing new methods to constrain the air-sea carbon flux from space will be necessary to quantify the impact of anthropogenic emissions reductions on atmospheric CO_2 mixing ratios.

Conclusions

The COVID-19 pandemic and associated changes in human behavior represent an unprecedented rapid change in anthropogenic emissions to the atmosphere. Due to the large differences in relevant atmospheric lifetimes for constituents central to AQ and climate, clear changes in local AQ but not global GHG trajectories were observed. Changes in AQ were very spatially heterogeneous, demonstrating that the same strategies to improve AQ do not apply equally well to all regions. Additionally, changes in AQ in the Los Angeles Basin correlated with temperature, precipitation, and severe wildfires, indicating that shifts in these quantities associated with climate change will at least partially offset gains in AQ made from past and future reductions in anthropogenic emissions.

Despite large disruptions in transportation emissions sectors, the global-scale change in the CO_2 growth rate was less than interannual variability. This is due to a combination of reduced ocean uptake of CO_2, a recovery of CO_2 emissions in the second half of 2020, and large interannual variability in land carbon fluxes. That recovery indicates that expecting changes to individual behavior to be sufficient to halt the increase of GHGs in the atmosphere is unrealistic. Instead, incentives to deploy new methods to systematically and sustainably reduce carbon intensity are needed. Given the bidirectional feedback between climate and AQ, it is clear that climate and AQ can no longer be considered separate problems; prompt action to reduce anthropogenic carbon emissions is essential not only to

⁶²⁹ avert direct climate impacts, but to avoid giving up decades
⁶³⁰ of hard-won progress in improving urban AQ.

Materials and Methods

⁶³² Full methods are available in the SI. Analysis of LA Basin AQ used
⁶³³ data from CA Air Resources Board monitors, filtered for complete
⁶³⁴ data records in the 2015 to 2020 period. 1 h daily maximum (DM)
⁶³⁵ NO_2 and temperature, 8 h DM O_3, and 24 h average PM were
⁶³⁶ calculated from this data. OPE was derived from model simulations
⁶³⁷ using multiconstituent assimilation of multiple satellite measure-
⁶³⁸ ments in the MIROC-CHASER model (32). OPE calculated by
⁶³⁹ comparing modeled O_3 production and NO_x emission difference be-
⁶⁴⁰ tween baseline (2010 to 2019) and reduced 2020 emissions. Separate
⁶⁴¹ $PM_{2.5}$ simulations used GEOS-Chem v9-02 with NO_x emissions
⁶⁴² consistent with the OPE simulations: baseline NO_x emissions used
⁶⁴³ HTAP v2 scaled to 2017 using satellite-derived emissions reduction
⁶⁴⁴ ratios and COVID NO_x emissions were scaled down by the same
⁶⁴⁵ factor as in the OPE simulations. The TROPOMI timeseries analy-
⁶⁴⁶ sis first regridded native TROPOMI pixels to a $0.01° \times 0.01°$ grid
⁶⁴⁷ and filtered to primarily remove cloud and snow/ice contaminated
⁶⁴⁸ scenes. The timeseries show the 75th percentile of 15-day rolling
⁶⁴⁹ average NO_2 columns in a $1° \times 1°$ box around each city.

⁶⁵⁰ Global CO_2 emissions estimates were derived from an array of
⁶⁵¹ near-real time data on power generation, industry, transport, and
⁶⁵² fuel consumption. XCO_2 growth rates were derived from OCO-2 v10
⁶⁵³ ocean glint data and XCH_4 growth rates from TCCON GGG2014
⁶⁵⁴ data. The data shown are 15-day running averages deseasonalized by
⁶⁵⁵ fitting a four-harmonic curve. Expected CH_4 trends we computed
⁶⁵⁶ from a two-box model (representing the two hemispheres) using
⁶⁵⁷ prescribed OH concentrations and constant CH_4 emissions after
⁶⁵⁸ 2012. TCCON data can be obtained from the TCCON Data Archive
⁶⁵⁹ hosted by CaltechDATA (https://tccondata.org./). The authors thank
⁶⁶⁰ the TCCON science team for their effort in providing this data.

⁶⁶¹ Publicly available datasets are listed along with data generated
⁶⁶² from this study and stored in public facing repositories in the SI,
⁶⁶³ table S1. Emissions data for Figs. 3 and 9 are given in Table S2.
⁶⁶⁴ Data for the OPE values in Fig. 7 is given in Table S4. Emissions
⁶⁶⁵ and OPE data also included as Excel SI files.

1. T Hale, et al., Oxford COVID-19 government response tracker. *Blavatnik School of Govern-* ⁶⁹⁴
   ment. (2020). ⁶⁹⁵
2. M Strohmeier, X Olive, J Lübbe, M Schäfer, V Lenders, Crowdsourced air traffic data from ⁶⁹⁶
   the OpenSky network 2019–20. *Earth Syst. Sci. Data Discuss.* **2020**, 1–15 (2020). ⁶⁹⁷
3. M Schäfer, M Strohmeier, V Lenders, I Martinovic, M Wilhelm, Bringing Up OpenSky: A Large- ⁶⁹⁸
   scale ADS-B Sensor Network for Research. *Proceedings of the 13th IEEE/ACM International* ⁶⁹⁹
   Symposium on Information Processing in Sensor Networks (IPSN), 83–94 (2014). ⁷⁰⁰
4. X Olive, traffic, a toolbox for processing and analysing air traffic data. *J. Open Source Softw.* ⁷⁰¹
   4 (2019). ⁷⁰²
5. C Lamprecht, M Graus, M Striednig, M Stichaner, T Karl, Decoupling of urban CO_2 and ⁷⁰³
   air pollutant emission reductions during the european SARS-CoV-2 lockdown. *Atmospheric* ⁷⁰⁴
   Chem. Phys. **21**, 3091–3102 (2021). ⁷⁰⁵
6. DL Goldberg, et al., Disentangling the impact of the COVID-19 lockdowns on urban NO_2 ⁷⁰⁶
   from natural variability. *Geophys. Res. Lett.* **47** (2020). ⁷⁰⁷
7. K Miyazaki, et al., Global tropospheric ozone responses to reduced NO_x emissions linked to ⁷⁰⁸
   the COVID-19 world-wide lockdowns. *Sci. Adv.* **7**, eabf7460 (2021). ⁷⁰⁹
8. CA Keller, et al., Global impact of covid-19 restrictions on the surface concentrations of nitro- ⁷¹⁰
   gen dioxide and ozone. *Atmospheric Chem. Phys.* **21**, 3555–3592 (2021). ⁷¹¹
9. J Xing, et al., Quantifying the emission changes and associated air quality impacts during ⁷¹²
   the COVID-19 pandemic on the north china plain: a response modeling study. *Atmospheric* ⁷¹³
   Chem. Phys. **20**, 14347–14359 (2020). ⁷¹⁴
10. M Guevara, et al., Time-resolved emission reductions for atmospheric chemistry modelling in ⁷¹⁵
    europe during the COVID-19 lockdowns. *Atmospheric Chem. Phys.* **21**, 773–797 (2021). ⁷¹⁶
11. T Doumbia, et al., Changes in global air pollutant emissions during the COVID-19 pandemic: ⁷¹⁷
    a dataset for atmospheric chemistry modeling. *Earth Syst. Sci. Data* (2021). ⁷¹⁸
12. International Energy Agency, Methane tracker 2021 (https://www.iea.org/reports/methane- ⁷¹⁹
    tracker-2021) (2021) last accessed 22 Apr 2021. ⁷²⁰
13. Z Liu, et al., Global daily CO_2 emissions for the year 2020 (2021). ⁷²¹
14. C Le Quéré, et al., Temporary reduction in daily global CO_2 emissions during the COVID-19 ⁷²²
    forced confinement. *Nat. Clim. Chang.* **10**, 647–653 (2020). ⁷²³
15. Z Liu, et al., Near-real-time monitoring of global CO_2 emissions reveals the effects of the ⁷²⁴
    COVID-19 pandemic (2020). ⁷²⁵
16. AJ Turner, et al., Observed impacts of COVID-19 on urban CO_2 emissions. *Geophys. Res.* ⁷²⁶
    Lett. **47**, e2020GL090037 (2020). ⁷²⁷
17. D Liu, et al., Observed decreases in on-road co$_2$ concentrations in beijing during covid-19. ⁷²⁸
    Atmospheric Chem. Phys. Discuss. **2020**, 1–18 (2020). ⁷²⁹
18. M Buchwitz, et al., Can a regional-scale reduction of atmospheric co$_2$ during the covid-19 ⁷³⁰
    pandemic be detected from space? a case study for east china using satellite xco$_2$ retrievals. ⁷³¹
    Atmospheric Meas. Tech. **14**, 2141–2166 (2021). ⁷³²
19. RM Duren, et al., California's methane super-emitters. *Nature* **575**, 180–184 (2019). ⁷³³
20. BK Lamb, et al., Direct measurements show decreasing methane emissions from natural gas ⁷³⁴
    local distribution systems in the united states. *Environ. Sci. & Technol.* **49**, 5161–5169 (2015). ⁷³⁵
21. DR Lyon, et al., Concurrent variation in oil and gas methane emissions and oil price during ⁷³⁶
    the COVID-19 pandemic. *Atmospheric Chem. Phys.* **21**, 6605–6626 (2021). ⁷³⁷
22. National Oceanic and Atmospheric Administration, Annual mean global carbon dioxide ⁷³⁸
    growth rates (https://www.esrl.noaa.gov/gmd/ccgg/trends/gl_gr.html) (2021) last accessed 26 ⁷³⁹
    Apr 2021. ⁷⁴⁰
23. T Shiraishi, R Hirata, Estimation of carbon dioxide emissions from the megafires of australia ⁷⁴¹
    in 2019–2020. *Sci. Reports* **11** (2021). ⁷⁴²
24. JC Fyfe, et al., Quantifying the influence of short-term emission reductions on climate. *Sci.* ⁷⁴³
    Adv. **7** (2021). ⁷⁴⁴
25. NS Lovenduski, et al., The ocean carbon response to COVID-related emissions reductions. ⁷⁴⁵
    Geophys. Res. Lett. **48** (2021). ⁷⁴⁶
26. D Wunch, et al., The Total Carbon Column Observing Network. *Philos. Transactions Royal* ⁷⁴⁷
    Soc. A: Math. Phys. Eng. Sci. **369**, 2087–2112 (2011). ⁷⁴⁸
27. D Wunch, et al., The Total Carbon Column Observing Network's GGG2014 data version, ⁷⁴⁹
    Technical report (2015). ⁷⁵⁰
28. PO Wennberg, et al., TCCON data from Park Falls (US), Release GGG2014R0 (TCCON ⁷⁵¹
    data archive, hosted by CaltechDATA) (2014). ⁷⁵²
29. V Sherlock, et al., TCCON data from Lauder (NZ), 125HR, Release GGG2014R0 (TCCON ⁷⁵³
    data archive, hosted by CaltechDATA) (2014). ⁷⁵⁴
30. DF Pollard, J Robinson, H Shiona, TCCON data from Lauder (NZ), Release GGG2014.R0 ⁷⁵⁵
    (TCCON data archive, hosted by CaltechDATA) (2019). ⁷⁵⁶
31. National Oceanic and Atmospheric Administration, Despite pandemic shutdowns, carbon ⁷⁵⁷
    dioxide and methane surged in 2020 (https://research.noaa.gov/article/ArtMID/587/ArticleID/ ⁷⁵⁸
    2742/Despite-pandemic-shutdowns-carbon-dioxide-and-methane-surged-in-2020) (2021) ⁷⁵⁹
    last accessed 26 Apr 2021. ⁷⁶⁰
32. K Miyazaki, et al., Updated tropospheric chemistry reanalysis and emission estimates, TCR- ⁷⁶¹
    2, for 2005–2018. *Earth Syst. Sci. Data* **12**, 2223–2259 (2020). ⁷⁶²
33. AJ Turner, C Frankenberg, EA Kort, Interpreting contemporary trends in atmospheric ⁷⁶³
    methane. *Proc. Natl. Acad. Sci.* **116**, 2805–2813 (2019). ⁷⁶⁴
34. Y Zhao, et al., Substantial changes in nitrogen dioxide and ozone after excluding meteorolog- ⁷⁶⁵
    ical impacts during the COVID-19 outbreak in mainland china. *Environ. Sci. Technol. Lett.* **7**, ⁷⁶⁶
    402–408 (2020). ⁷⁶⁷
35. SK Grange, et al., Covid-19 lockdowns highlight a risk of increasing ozone pollution in euro- ⁷⁶⁸
    pean urban areas. *Atmospheric Chem. Phys.* **21**, 4169–4185 (2021). ⁷⁶⁹
36. JD Lee, WS Drysdale, DP Finch, SE Wilde, PI Palmer, UK surface NO_2 levels dropped by ⁷⁷⁰
    42 % during the COVID-19 lockdown: impact on surface O_3. *Atmospheric Chem. Phys.* **20**, ⁷⁷¹
    15743–15759 (2020). ⁷⁷²
37. P Messina, et al., Global biogenic volatile organic compound emissions in the ORCHIDEE ⁷⁷³
    and MEGAN models and sensitivity to key parameters. *Atmospheric Chem. Phys.* **16**, 14169– ⁷⁷⁴
    14202 (2016). ⁷⁷⁵
38. HA Parker, S Hasheminassab, JD Crounse, CM Roehl, PO Wennberg, Impacts of traffic ⁷⁷⁶
    reductions associated with COVID-19 on Southern California air quality. *Geophys. Res. Lett.* ⁷⁷⁷
    47 (2020). ⁷⁷⁸
39. C Ivey, et al., Impacts of the 2020 COVID-19 Shutdown Measures on Ozone Production in ⁷⁷⁹
    the Los Angeles Basin, preprint (2020). ⁷⁸⁰
40. DJ Rasmussen, J Hu, A Mahmud, MJ Kleeman, The ozone–climate penalty: Past, present, ⁷⁸¹

782   and future. *Environ. Sci. & Technol.* **47**, 14258–14266 (2013).

783   41. U.S. EPA, Integrated science assessment (ISA) for particulate matter, (U.S. Environmental
784   Protection Agency, Washington, D.C.), Technical Report EPA/600/R-19/188 (2019).

785   42. AS Ansari, SN Pandis, Response of inorganic PM to precursor concentrations. *Environ. Sci.*
786   *& Technol.* **32**, 2706–2714 (1998).

787   43. MS Hammer, et al., Effects of COVID-19 lockdowns on fine particular matter concentrations.
788   *Sci. Adv.* (in press).

789   44. JD Berman, K Ebisu, Changes in U.S. air pollution during the COVID-19 pandemic. *Sci. The*
790   *Total. Environ.* **739**, 139864 (2020).

791   45. Z Zheng, G Xu, Q Li, C Chen, J Li, Effect of precipitation on reducing atmospheric pollutant
792   over Beijing. *Atmospheric Pollut. Res.* **10**, 1443–1453 (2019).

793   46. X Zhao, Y Sun, C Zhao, H Jiang, Impact of precipitation with different intensity on PM2.5 over
794   typical regions of China. *Atmosphere* **11**, 906 (2020).

795   47. Z Jiang, et al., Unexpected slowdown of US pollutant emission reduction in the past decade.
796   *Proc. Natl. Acad. Sci.* **115**, 5099–5104 (2018).

797   48. JL Laughner, RC Cohen, Direct observation of changing NO_x lifetime in North American
798   cities. *Science* **366**, 723–727 (2019).

799   49. DT Shindell, Y Lee, G Faluvegi, Climate and health impacts of US emissions reductions
800   consistent with 2°C. *Nat. Clim. Chang.* **6**, 503–507 (2016).

801   50. SE Pusede, AL Steiner, RC Cohen, Temperature and recent trends in the chemistry of conti-
802   nental surface ozone. *Chem. Rev.* **115**, 3898–3918 (2015).

803   51. AP Williams, et al., Observed impacts of anthropogenic climate change on wildfire in califor-
804   nia. *Earth's Futur.* **7**, 892–910 (2019).

805   52. T Stocker, et al., Technical summary in *Climate Change 2013: The Physical Science Basis.*
806   *Contribution of Working Group I to the Fifth Assessment Report of the Intergovernmental*
807   *Panel on Climate Change*, eds. T Stocker, et al. (Cambridge University Press, Cambridge,
808   United Kingdom and New York, NY, USA), (2013).

809   53. S Ridge, G McKinley, Ocean carbon uptake under aggressive emission mitigation. *Biogeo-*
810   *sciences* **18**, 2711–2725 (2021).

811   54. L Brubaker, Women physicians and the COVID-19 pandemic. *JAMA* **324**, 835 (2020).

812   55. JLC Kok, Short-term trade-off between stringency and economic growth. *COVID Econ.* **60**,
813   172–189 (2020).

814   56. EB Barbier, Greening the post-pandemic recovery in the G20. *Environ. Resour. Econ.* **76**,
815   685–703 (2020).

816   57. Z Chen, G Marin, D Popp, F Vona, Green stimulus in a post-pandemic recovery: the role of
817   skills for a resilient recovery. *Environ. Resour. Econ.* **76**, 901–911 (2020).